Ultrashort Near-Infrared Fiber-Optic Sensors for Carbon Dioxide Detection

Citation	Chong, X., Kim, K. J., Ohodnicki, P., Li, E., Chang, C. H., & Wang, A. (2015). Ultra-Short Near-Infrared Fiber-Optic Sensors for Carbon Dioxide Detection. IEEE Sensors Journal, 15(9), 5327-5332. doi:10.1109/JSEN.2015.2438063
DOI	10.1109/JSEN.2015.2438063
Publisher	Institute of Electrical and Electronics Engineers
Version	Version of Record
Terms of Use	http://cdss.library.oregonstate.edu/sa-termsofuse

Ultrashort Near-Infrared Fiber-Optic Sensors for Carbon Dioxide Detection

Xinyuan Chong, *Student Member, IEEE*, Ki-Joong Kim, Paul R. Ohodnicki, Erwen Li, Chih-Hung Chang, *Member, IEEE*, and Alan X. Wang, *Senior Member, IEEE*

***Abstract*— In this paper, we report a fiber-optic carbon dioxide (CO_2) near-infrared (IR) absorption sensor with only 8-cm sensing length that is coated with nanoporous metal-organic framework material Cu-BTC (BTC = benzene-1,3, 5-tricarboxylate). The multimode optical fiber was etched by hydrofluoric acid to remove the cladding and part of the core, resulting in larger evanescent field to sense the near-IR absorption induced by the adsorbed CO_2. The Cu-BTC thin film with 100 nm thickness was then grown onto the ethced core through a stepwise layer-by-layer method. Our real-time measurement results show that the CO_2 detection limit is better than 500 ppm and the overall response time is 40 s for absorption and 75 s for desorption. To the best of our knowledge, this is the shortest near-IR fiber-optic sensor for CO_2 detection at 1.57-μm wavelength.**

***Index Terms*— Fiber optic sensor, gas sensor, near infrared absorption, metal-organic framework.**

I. Introduction

FIBER-OPTIC sensors are playing significant roles in many engineering applications due to the unique advantages such as light weight, low cost, compact size, immunity to electromagnetic interference, and large communication bandwidth [1]. Various sensing technologies have been developed [2]–[7], of which fiber-optic evanescent field sensor [6] is one of the most established and widely used techniques that can offer exclusive advantages of easy optical coupling and excellent capabilities for distributed sensing and sensor network. A broad spectrum of applications have been reported including chemical sensing [2], [8], [9], gas sensing [4]–[6], [10]–[16], and biosensing [3], [17], [18]. Since this sensing mechanism relies on the penetration of the evanescent field of a total internally reflected light into the absorbing medium (cladding layer), it suffers low sensitivity due to the small percentage of the optical power carried by the evanescent field when compared with hollow core or micro-structured fibers [6]. This issue becomes even worse for gas sensing due to the low molecule density. Compared with infrared (IR) absorption through a gas cell, the sensitivity of an equivalent length evanescent field fiber-optic sensor is typically three to four orders of magnitude lower [15]. This may not be a serious issue for mid-IR (2.5-10 μm wavelength) sensors that work at the highly absorptive fundamental vibrational bands [19]. However, most commercial mid-IR spectrometers are expensive, large, and heavy tabletop instrument that is unsuitable for mobile or distributed sensing applications. On the other hand, optical communication systems for telecom industry have enabled near-infrared (NIR) optical fibers and optoelectronic devices that are miniaturized, low cost, and highly reliable during last a few decades, which has significantly accelerated the development of NIR sensors [20]–[23]. The biggest challenge is that most gases do not have fundamental vibration bands at NIR regions. The absorptions have to come from overtunes of the fundamental vibration bands, and hence it has relatively low detection sensitivity. Therefore, evanescent field NIR fiber-optic gas sensors typically must be several meters in length in order to achieve acceptable sensitivity.

To resolve this challenge, we develop ultra-short NIR fiber-optic gas sensors for carbon dioxide (CO_2) detection by depositing a thin layer of metal-organic framework (MOF) on the core of multimode fibers. MOF is a new class of highly porous crystalline material consisting of metal ions and bridging organic ligands linked together by coordination bonds. Due to its high surface area, chemical and physical tailorability and tunable nanostructured cavities, it has been widely applied in chemical separation [24]–[26], gas storage [27]–[30], drug delivery [31]–[33], sensing [34]–[37], and catalysis applications [38]–[40]. In our NIR fiber-optic sensors, the 100 nm thick MOF film coated at the surface of the fiber core absorbs CO_2 in the ambient environment, and effectively increases the local CO_2 concentration at the surface of the optical fiber, which essentially enhances the interaction between the evanescent field and the gas analyte. As a result, we successfully increased the NIR detection sensitivity with an ultra-short length.

II. Preparation of MOF-Coated NIR Fiber Optic Sensors

The evanescent field NIR fiber-optic sensor was fabricated by growing nanoporous MOF materials on the core sur-

Manuscript received December 21, 2014; revised May 15, 2015; accepted May 15, 2015. Date of publication June 1, 2015; date of current version July 24, 2015. This work was supported by the National Energy Technology Laboratory's ongoing research through RES under Contract DE-FE0004000. The associate editor coordinating the review of this paper and approving it for publication was Dr. Anna G. Mignani. *(Xinyuan Chong and Ki-Joong Kim contributed equally to this work.) (Corresponding author: Chih-Hung Chang and Alan X. Wang.)*

X. Chong, E. Li, and A. X. Wang are with the School of Electrical Engineering and Computer Science, Oregon State University, Corvallis, OR 97331 USA (e-mail: chongx@onid.oregonstate.edu; lie@onid.oregonstate.edu; wang@eecs.oregonstate.edu).

K.-J. Kim and C.-H. Chang are with the School of Chemical, Biological Environmental Engineering, Oregon State University, Corvallis, OR 97331 USA (e-mail: goldcat.kjkim@gmail.com; chih-hung.chang@oregonstate.edu).

P. R. Ohodnicki is with the National Energy Technology Laboratory, U.S. Department of Energy, Pittsburgh, PA 15236 USA (e-mail: paul.ohodnicki@netl.doe.gov).

Color versions of one or more of the figures in this paper are available online at http://ieeexplore.ieee.org.

Digital Object Identifier 10.1109/JSEN.2015.2438063

face of a multimode fiber (MMF). First, standard buffered oxide etchant (BOE) was used to etch away the cladding of a fluorine-doped silica cladded/silica core MMF (Thorlabs AFS 105/125Y). The length of the etched region is about 8 cm. Prior to the etching process, the MMF polymer coating layer was removed by chemical stripping over a slightly longer length of about 10 cm. To increase the interaction between the evanescent field and the surrounding gas molecules and thereby enhance the sensitivity, the 125 μm core of the MMF was etched to approximately 75 μm. Second, the etched fiber was cleaned thoroughly by acetone, isopropanol and deionized water, respectively, followed by O_2 plasma treatment (50 w) for 20 min. Finally, a MOF thin layer was grown on the surface of the etched core by stepwise layer-by-layer (LBL) method [41]. Briefly, the fiber was first immersed into a 300 mL ethanol solution which contains 10 mM metal precursor $Cu(Ac)_2$ for 20 min. Subsequently, the MMF was immersed into another 300 mL ethanol solution which contains 1 mM organic ligand benzene-1,3,5-tricarboxylate (BTC) for 40 min. Between each step, the fiber was rinsed with ethanol to remove the unreacted precursor ions or molecules to ensure the uniform growth and then naturally dried at room temperature for 10 min. Optical microscopy images of the MMF before and after growing MOF are shown in Figure 1 (a) and (b). The silica core of the MMF was coated with MOF which shows a light blue color due to the copper ions. The scanning electron microscopy (SEM) images of the MOF-coated MMF are shown in Figure 1 (c) and (d). The cross sectional SEM image in Figure 1 (c) indicates that the thickness of the MOF film with 100 nm was obtained by 30 cycles LBL growth, and the top SEM image with a tilted perspective angle in Figure 1 (d) shows that the MOF film consists of many single crystals with average size less than 1μm. In addition, we did not observe any peel-off of the MOF film from the MMF, indicating good bonding between these two materials. The XRD pattern of the MOF-coated MMF [the upper curve of Figure 1 (e)] shows only one peak at $2\theta = 11.6°$, corresponding to the (222) plane of Cu-BTC. This indicates the highly oriented growth, having a hexagonal shaped unit cell viewed along the (111) direction [42], compared to that of the polycrystalline bulk Cu-BTC prepared by solvothermal method [the lower curve of Figure 1 (e)]. This might due to the presence of -OH functional groups on the surface of optical fibers after O_2 plasma treatment, leading to preferentially oriented films [43].

MOFs are relatively new materials, and most optical characterizations of MOF are focused in the visible wavelength range. For example, it has been confirmed that the organic ligands will induce optical absorption between 400 and 800 nm [44]. To measure the optical properties of MOF in the NIR wavelength range, a 100 nm thick MOF film was grown on a silicon wafer with 10 nm silicon oxide top layer. The refractive indices of the MOF film were measured and modeled using ellipsometry as shown in Figure 2. The real part of the refractive index of MOF is 1.33 at 1.57 μm wavelength with a small dispersion from 1.1 to 1.7 μm. The imaginary part of the refractive index is negligible, which means that there is no material absorption in the NIR wavelength range, which is very critical for NIR absorption sensing. The refractive index

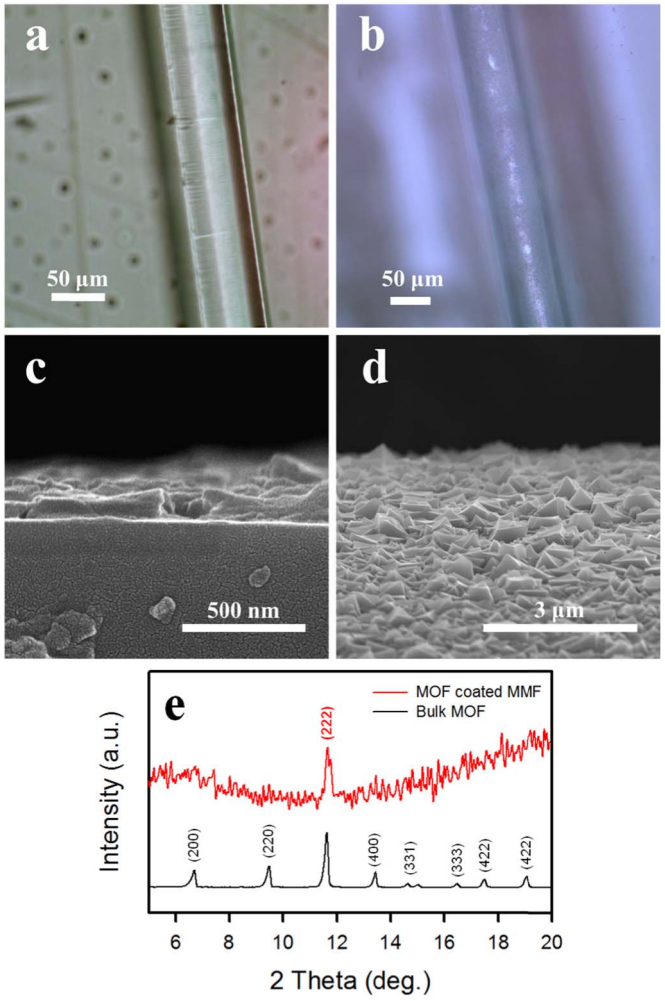

Fig. 1. Optical images of the core of MMF (a) before and (b) after coating MOF. (c) Cross-sectional and (d) top SEM images of the MOF-coated MMF after 30 cycles LBL growth. (e) XRD patterns of the MOF-coated MMF and bulk MOF prepared by typical solvothermal method.

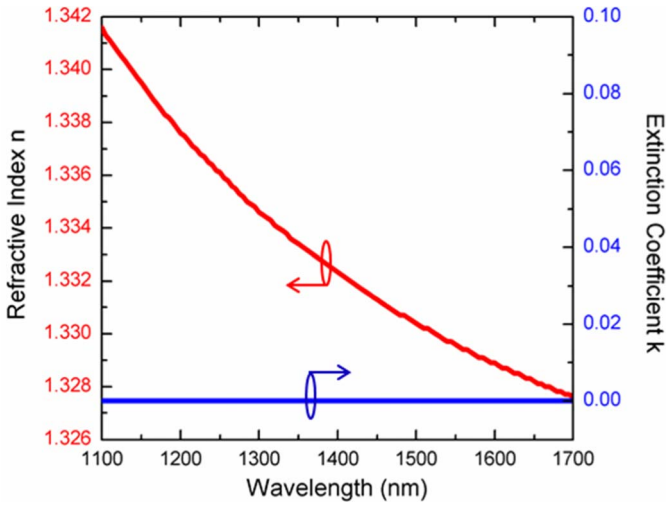

Fig. 2. Refractive index n and extinction coefficient k of MOF measured by ellipsometry.

of MOF is less than that of the MMF core (1.45) but greater than that of air, therefore, light can still propagate inside the MMF core, while the evanescent field will also be enhanced compared with air cladding.

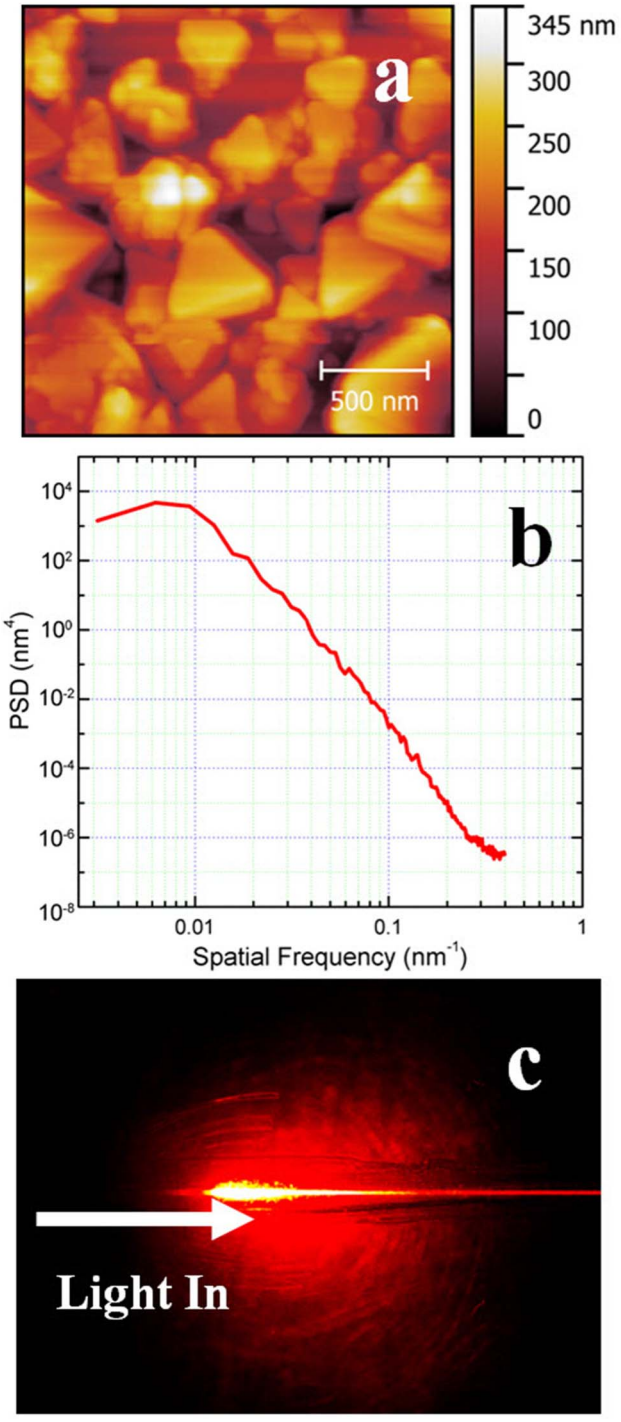

Fig. 3. (a) AFM image of MMF coated with MOF; (b) FFT of the surface profile in the spatial domain; and (c) Optical scattering image of the MOF-coated fiber-optic sensor illuminated by a 635 nm red laser.

The major optical loss of the fiber-optic gas sensors is caused by the surface roughness of the MOF crystals as shown in Figure 1 (d). Quantitative measurement of the fiber-optic sensor surface profile was conducted by atomic force microscopy (AFM) as shown in Figure 3 (a). The AFM surface profile corresponds very well with the SEM image in Figure 1(d), with clear images of the small MOF crystals. The root mean square of the surface profile is 64.1nm. Since the optical scattering strongly depends on the spatial frequency of the surface profile, post-measurement analysis using fast Fourier transform (FFT) was executed and the results are shown in Figure 3 (b). In our AFM image, the scanning area is 2 μm $\times$ 2 μm with 8 nm spatial resolution. The plotted spatial frequencies from 0.003 nm^{-1} to 0.4 nm^{-1} show peak power spectral density (PSD) at 0.006 nm^{-1}, which corresponds to the average MOF crystal size. Surface roughness with such spatial frequencies is comparable with the NIR wavelength in the fiber and should cause significant amount of optical scattering. The optical image of the MOF-coated MMF illuminated by a 635 nm semiconductor laser in Figure 3 (c) confirms the strong optical scattering. We also coupled broadband NIR light (1.5-1.6 μm) from an amplified spontaneous emission (ASE) light source into the fiber-optic sensor. The total loss for the MMF without MOF was 6.8 dB. After being coated with MOF, the loss increased to 15.8 dB.

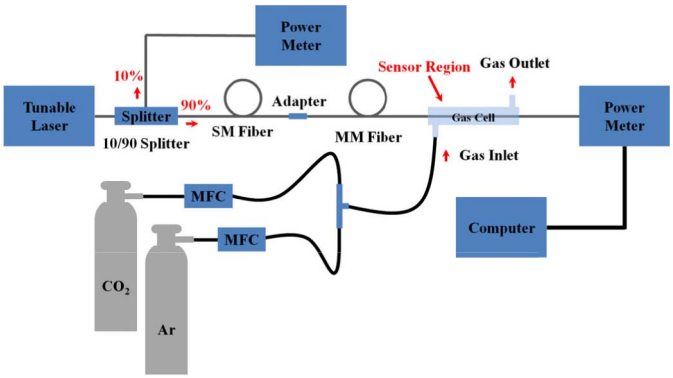

Fig. 4. Schematic of the experiment setup for CO_2 sensing.

III. Experiment Setup for CO_2 Sensing

The experiment setup for CO_2 sensing is shown in Figure 4. A tunable semiconductor laser diode (HP 8168) with a standard single mode (SMF28) fiber pigtail was used as the light source. The output light was first split by a 1×2 10:90 coupler. 10% of the light was coupled into a power meter (Thorlabs, Inc. PM20) as the reference, and the other 90% was coupled into the fiber-optic sensor by a buffered fiber adapter (FIS F18294). The sensor was placed inside a gas cell, which was connected to the CO_2 and Ar gas tanks. The transmitted light through the sensor was directly coupled to another power meter (Thorlabs, Inc. S122C), and the data was collected by a personal computer through a USB power and energy meter interface (Thorlabs, Inc. PM100USB). Gas flows were controlled by two mass flow controllers (MFC) (Aalborg, GFC 17) with 0-20 ml/min flow range. Different CO_2 concentration was achieved by varying the mixing ratio of CO_2 and Ar flows.

IV. Results and Discussions

The gas cell was first purged by ultra-pure Ar for 2 hours to remove water vapor inside the MOF. Then, the gas flow was switched from pure Ar to CO_2 with a flow rate of 5 sccm for 5 minutes. The wavelength of the tunable laser

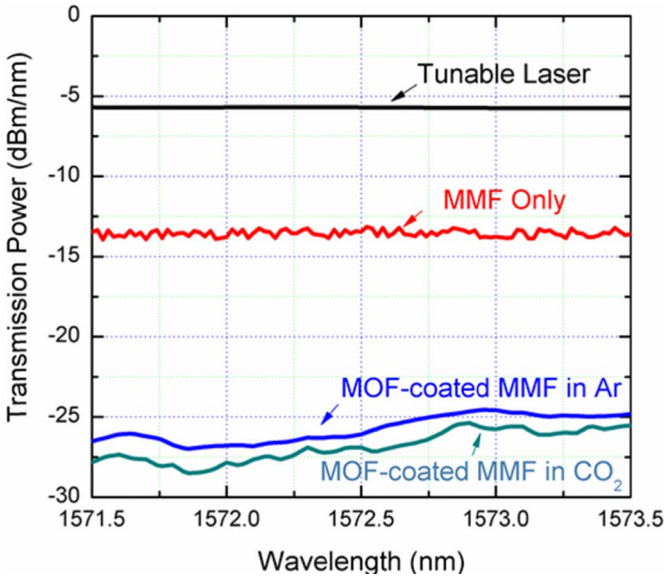

Fig. 5. Optical transmission spectra of the tunable laser, MMF, MOF-coated MMF in Ar and in CO_2, respectively.

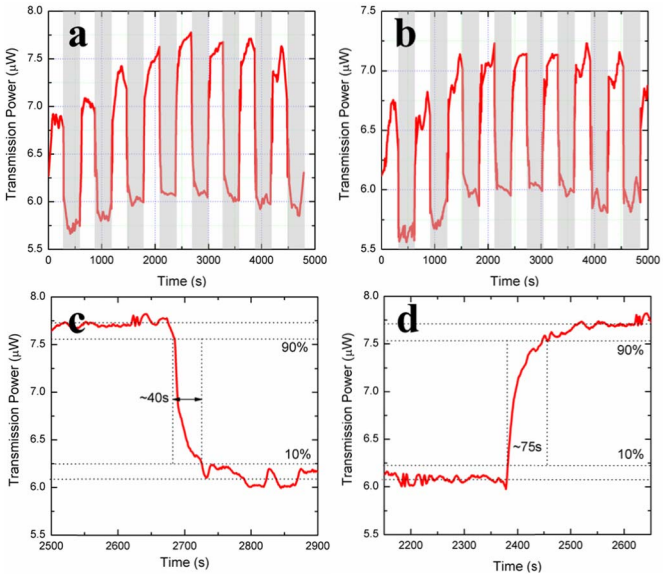

Fig. 6. Real-time response of the fiber-optic sensor to alternating Ar and CO_2 flows at (a) 1572.5 nm, (b) 1500 nm; Response time of the fiber-optic sensor for (c) absorbing and (d) desorbing CO_2.

was continuously scanned from 1571.5 nm to 1583.5 nm with 0.02 nm resolution. The optical transmission spectra of the tunable laser, MMF fiber only, MOF-coated MMF fiber with pure Ar and with pure CO_2 were plotted in Figure 5. Compared with the tunable laser, the MMF without MOF had 8 dB optical insertion loss due the optical coupling at the fiber connectors and the optical scattering caused by surface roughness at the sensing region. Also, the spectrum was no longer flat and smooth due to the modal noise of MMF. After coated with MOF and purged with Ar, the optical loss further increased to 21 dB due to extra optical scattering by MOF. When switched the gas flow to pure CO_2, the optical transmission spectra dropped around 1 dB due to the CO_2 absorption. As a comparison, if the MMF is not coated with MOF, switching Ar to CO_2 will not induce any observable change of the optical transmission since the fiber is not long enough to induce detectable NIR absorption.

To further study the dynamic response, real-time data of the fiber-optic sensor was measured. The wavelength of the tunable laser was fixed at 1572.5 nm. Then, pure Ar and CO_2 gas flows were switched alternately every 5 minutes. In Figure 6(a), the grey regions and white regions represent the time slots when CO_2 and Ar flows, respectively. The average transmission power difference between flowing Ar and CO_2 is about 1.6 μW. As a comparison, the absorption measurement was repeated at 1500 nm in Figure 6(b) with average absorption around 1.1 μW. This observation implies that the absorption spectrum of CO_2 in MOF might be different from the gas in free space, which should have orders of magnitude higher absorption rate in the 1572.5 nm absorption lines than in 1500 nm. Interestingly, when we used 635 nm laser diode as the light source, we did not observe any meaningful absorption. Our results confirmed that the optical absorption at 1572.5 nm and 1500 nm were caused by the CO_2 absorption in MOF, which may have different spectral widths than the a few narrow lines as predicted by HITRAN [45]. The response

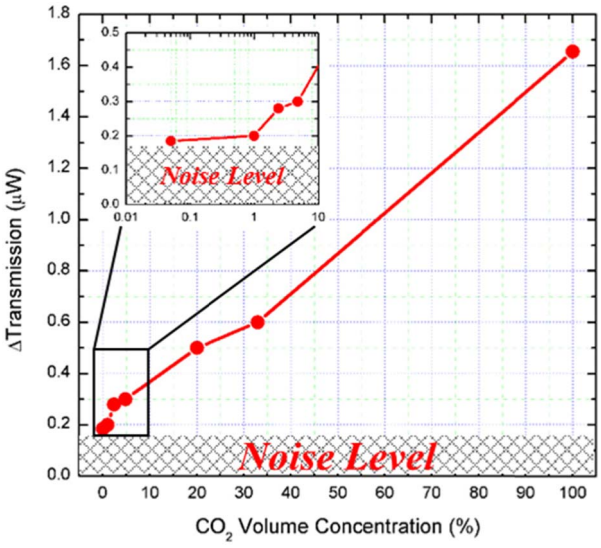

Fig. 7. Average ΔTransmission as a function of CO_2 volume concentration in Ar. Inset: zoomed-in plot for low concentration (log scale).

time of the sensor was measured for both the absorption and desorption process as shown in Figure 6(c) and (d). The absorption time (from 90% to 10%) was approximately 40 seconds and the desorption time (from 10% to 90%) was approximately 75 seconds. It should be noticed that these results the overall response times including purging the gas cell with volume of 7 cm^3. The MOF layer is only 100 nm thick, and the absorption time and desorption time for CO_2 is therefore likely to be negligible compared with the time to purge the gas cell.

The detection limit of the fiber-optic sensor was tested by measuring the change of the transmitted optical power (ΔTransmission) as a function of CO_2 concentration. Different CO_2 concentrations were obtained by controlling the flow rates of pure Ar and CO_2. From the plot of Figure 7,

we can clearly observe the relation between ΔTransmission and the CO_2 concentration. The slope at higher concentration (>5%) is smaller than that at lower CO_2 concentration. This is because higher concentration CO_2 will saturate the nanoporous MOF film, which is consistent with the reported results [46]. The inset figure shows zoomed-in plot of ΔTransmission vs. CO_2 volume concentration in log-scale. The lowest CO_2 concentration we measured is 500 ppm, which is limited by the noise of the MMF, which caused signal fluctuation that is comparable with low concentration CO_2 absorption. Using a single-mode optical fiber coated with MOF should further improve the detection limit.

V. Conclusion

In summary, we have developed ultra-short NIR fiber-optic gas sensors based on MOF-coated MMF for CO_2 sensing. Compared with conventional evanescent field fiber-optic gas sensors, the sensing length was reduced to only 8 cm by selective concentration of CO_2 into the MOF layer that was coated at the surface of the core of the MMF. We achieved a detection limit of 500 ppm, and the overall real-time response was found to be only 40 seconds for absorption and 75 seconds for desorption in a gas cell designed in this study. To the best of our knowledge, this is the shortest NIR fiber-optic sensor for CO_2 detection at 1.57μm wavelength. Such ultra-short fiber-optic gas sensors with rapid response time can be used for greenhouse gas detection and environmental protection.

References

[1] B. Lee, "Review of the present status of optical fiber sensors," *Opt. Fiber Technol.*, vol. 9, no. 2, pp. 57–79, Apr. 2003.

[2] J. H. Ahn, T. Y. Seong, W. M. Kim, T. S. Lee, I. Kim, and K.-S. Lee, "Fiber-optic waveguide coupled surface plasmon resonance sensor," *Opt. Exp.*, vol. 20, no. 19, pp. 21729–21738, Sep. 2012.

[3] M. H. Chiu, S. F. Wang, and R. S. Chang, "D-type fiber biosensor based on surface-plasmon resonance technology and heterodyne interferometry," *Opt. Lett.*, vol. 30, no. 3, pp. 233–235, Feb. 2005.

[4] O. Frazão, J. L. Santos, F. M. Araújo, and L. A. Ferreira, "Optical sensing with photonic crystal fibers," *Laser Photon. Rev.*, vol. 2, no. 6, pp. 449–459, Dec. 2008.

[5] N. Gayraud *et al.*, "Mid-infrared gas sensing using a photonic bandgap fiber," *Appl. Opt.*, vol. 47, no. 9, pp. 1269–1277, Mar. 2008.

[6] Y. L. Hoo, W. Jin, H. L. Ho, D. N. Wang, and R. S. Windeler, "Evanescent-wave gas sensing using microstructure fiber," *Opt. Eng.*, vol. 41, no. 1, pp. 8–9, Jan. 2002.

[7] W.-C. Lai, S. Chakravarty, X. Wang, C. Lin, and R. T. Chen, "On-chip methane sensing by near-IR absorption signatures in a photonic crystal slot waveguide," *Opt. Lett.*, vol. 36, no. 6, pp. 984–986, Mar. 2011.

[8] Z. L. Poole, P. Ohodnicki, R. Chen, Y. Lin, and K. P. Chen, "Engineering metal oxide nanostructures for the fiber optic sensor platform," *Opt. Exp.*, vol. 22, no. 3, pp. 2665–2674, Feb. 2014.

[9] M. R. R. Khan *et al.*, "Fiber-optic multi-sensor array for detection of low concentration volatile organic compounds," *Opt. Exp.*, vol. 21, no. 17, pp. 20119–20130, Aug. 2013.

[10] T. Ritari *et al.*, "Gas sensing using air-guiding photonic bandgap fibers," *Opt. Exp.*, vol. 12, no. 17, pp. 4080–4087, Aug. 2004.

[11] C.-L. Tien, H.-W. Chen, W.-F. Liu, S.-S. Jyu, S.-W. Lin, and Y.-S. Lin, "Hydrogen sensor based on side-polished fiber Bragg gratings coated with thin palladium film," *Thin Solid Films*, vol. 516, no. 16, pp. 5360–5363, Jun. 2008.

[12] P. R. Ohodnicki, Jr., M. Andio, and C. Wang, "Optical gas sensing responses in transparent conducting oxides with large free carrier density," *J. Appl. Phys.*, vol. 116, no. 2, p. 024309, Jul. 2014.

[13] J. Dai, M. Yang, X. Yu, and H. Lu, "Optical hydrogen sensor based on etched fiber Bragg grating sputtered with Pd/Ag composite film," *Opt. Fiber Technol.*, vol. 19, no. 1, pp. 26–30, Jan. 2013.

[14] P. R. Ohodnicki, M. P. Buric, T. D. Brown, C. Matranga, C. Wang, and J. Baltrus, "Plasmonic nanocomposite thin film enabled fiber optic sensors for simultaneous gas and temperature sensing at extreme temperatures," *Nanoscale*, vol. 5, no. 19, pp. 9030–9039, 2013.

[15] G. Stewart, F. A. Muhammad, and B. Culshaw, "Sensitivity improvement for evanescent-wave gas sensors," *Sens. Actuators B, Chem.*, vol. 11, nos. 1–3, pp. 521–524, Mar. 1993.

[16] A. S. Webb, F. Poletti, D. J. Richardson, and J. K. Sahu, "Suspended-core holey fiber for evanescent-field sensing," *Opt. Eng.*, vol. 46, no. 1, p. 010503, Jan. 2007.

[17] J. B. Jensen *et al.*, "Photonic crystal fiber based evanescent-wave sensor for detection of biomolecules in aqueous solutions," *Opt. Lett.*, vol. 29, no. 17, pp. 1974–1976, Sep. 2004.

[18] X. Fan, I. M. White, S. I. Shopova, H. Zhu, J. D. Suter, and Y. Sun, "Sensitive optical biosensors for unlabeled targets: A review," *Anal. Chim. Acta*, vol. 620, nos. 1–2, pp. 8–26, Jul. 2008.

[19] S. Herminjard *et al.*, "Surface plasmon resonance sensor showing enhanced sensitivity for CO_2 detection in the mid-infrared range," *Opt. Exp.*, vol. 17, no. 1, pp. 293–303, Jan. 2009.

[20] P. Werle, F. Slemr, K. Maurer, R. Kormann, R. Mücke, and B. Jänker, "Near- and mid-infrared laser-optical sensors for gas analysis," *Opt. Lasers Eng.*, vol. 37, nos. 2–3, pp. 101–114, Feb./Mar. 2002.

[21] H.-N. Li, D.-S. Li, and G.-B. Song, "Recent applications of fiber optic sensors to health monitoring in civil engineering," *Eng. Struct.*, vol. 26, no. 11, pp. 1647–1657, Sep. 2004.

[22] P. M. Nellen *et al.*, "Reliability of fiber Bragg grating based sensors for downhole applications," *Sens. Actuators A, Phys.*, vol. 103, no. 3, pp. 364–376, Feb. 2003.

[23] G. Stewart, W. Jin, and B. Culshaw, "Prospects for fibre-optic evanescent-field gas sensors using absorption in the near-infrared," *Sens. Actuators B, Chem.*, vol. 38, nos. 1–3, pp. 42–47, Jan./Feb. 1997.

[24] J. R. Li, J. Sculley, and H. C. Zhou, "Metal-organic frameworks for separations," *Chem. Rev.*, vol. 112, no. 2, pp. 869–932, Feb. 2012.

[25] J. S. Seo *et al.*, "A homochiral metal–organic porous material for enantioselective separation and catalysis," *Nature*, vol. 404, no. 6781, pp. 982–986, Apr. 2000.

[26] S.-C. Xiang *et al.*, "Rationally tuned micropores within enantiopure metal-organic frameworks for highly selective separation of acetylene and ethylene," *Nature Commun.*, vol. 2, p. 204, Feb. 2011.

[27] N. L. Rosi *et al.*, "Hydrogen storage in microporous metal-organic frameworks," *Science*, vol. 300, no. 5622, pp. 1127–1129, May 2003.

[28] M. P. Suh, H. J. Park, T. K. Prasad, and D. W. Lim, "Hydrogen storage in metal-organic frameworks," *Chem. Rev.*, vol. 112, no. 2, pp. 782–835, Feb. 2012.

[29] Y.-S. Bae and R. Q. Snurr, "Development and evaluation of porous materials for carbon dioxide separation and capture," *Angewandte Chem. Int. Ed.*, vol. 50, no. 49, pp. 11586–11596, 2011.

[30] K. Sumida *et al.*, "Carbon dioxide capture in metal-organic frameworks," *Chem. Rev.*, vol. 112, no. 2, pp. 724–781, Feb. 2012.

[31] P. Horcajada *et al.*, "Porous metal-organic-framework nanoscale carriers as a potential platform for drug delivery and imaging," *Nature Mater.*, vol. 9, no. 2, pp. 172–178, Feb. 2010.

[32] P. Horcajada *et al.*, "Flexible porous metal-organic frameworks for a controlled drug delivery," *J. Amer. Chem. Soc.*, vol. 130, no. 21, pp. 6774–6780, May 2008.

[33] J. Della Rocca, D. Liu, and W. Lin, "Nanoscale metal–organic frameworks for biomedical imaging and drug delivery," *Accounts Chem. Res.*, vol. 44, no. 10, pp. 957–968, Oct. 2011.

[34] L. E. Kreno, K. Leong, O. K. Farha, M. Allendorf, R. P. Van Duyne, and J. T. Hupp, "Metal–organic framework materials as chemical sensors," *Chem. Rev.*, vol. 112, no. 2, pp. 1105–1125, Feb. 2012.

[35] T.-H. Yu, C.-H. Ho, C.-Y. Wu, C.-H. Chien, C.-H. Lin, and S. Lee, "Metal–organic frameworks: A novel SERS substrate," *J. Raman Spectrosc.*, vol. 44, no. 11, pp. 1506–1511, Nov. 2013.

[36] Y. Hu, J. Liao, D. Wang, and G. Li, "Fabrication of gold nanoparticle-embedded metal–organic framework for highly sensitive surface-enhanced Raman scattering detection," *Anal. Chem.*, vol. 86, no. 8, pp. 3955–3963, Apr. 2014.

[37] R. J. T. Houk *et al.*, "Silver cluster formation, dynamics, and chemistry in metal-organic frameworks," *Nano Lett.*, vol. 9, no. 10, pp. 3413–3418, Oct. 2009.

[38] J. Lee, O. K. Farha, J. Roberts, K. A. Scheidt, S. T. Nguyen, and J. T. Hupp, "Metal–organic framework materials as catalysts," *Chem. Soc. Rev.*, vol. 38, no. 5, pp. 1450–1459, 2009.

[39] M. Yoon, R. Srirambalaji, and K. Kim, "Homochiral metal-organic frameworks for asymmetric heterogeneous catalysis," *Chem. Rev.*, vol. 112, no. 2, pp. 1196–1231, Feb. 2012.

[40] D. Dang, P. Wu, C. He, Z. Xie, and C. Duan, "Homochiral metal-organic frameworks for heterogeneous asymmetric catalysis," *J. Amer. Chem. Soc.*, vol. 132, no. 41, pp. 14321–14323, Oct. 2010.
[41] O. Shekhah *et al.*, "Step-by-step route for the synthesis of metal-organic frameworks," *J. Amer. Chem. Soc.*, vol. 129, no. 49, pp. 15118–15119, Dec. 2007.
[42] S. S.-Y. Chui, S. M.-F. Lo, J. P. H. Charmant, A. G. Orpen, and I. D. Williams, "A chemically functionalizable nanoporous material $[Cu_3(TMA)_2(H_2O)_3]_n$," *Science*, vol. 283, no. 5405, pp. 1148–1150, Feb. 1999.
[43] K.-J. Kim *et al.*, "Plasmonics-enhanced metal–organic framework nanoporous films for highly sensitive near-infrared absorption," *J. Mater. Chem. C*, vol. 3, no. 12, pp. 2763–2767, 2015.
[44] M. A. Nasalevich, M. G. Goesten, T. J. Savenije, F. Kapteijn, and J. Gascon, "Enhancing optical absorption of metal–organic frameworks for improved visible light photocatalysis," *Chem. Commun.*, vol. 49, no. 90, pp. 10575–10577, 2013.
[45] L. S. Rothman *et al.*, "The HITRAN2012 molecular spectroscopic databases," *J. Quant. Spectrosc. Radiat. Transf.*, vol. 130, pp. 4–50, Nov. 2013.
[46] A. R. Millward and O. M. Yaghi, "Metal-organic frameworks with exceptionally high capacity for storage of carbon dioxide at room temperature," *J. Amer. Chem. Soc.*, vol. 127, no. 51, pp. 17998–17999, Dec. 2005.

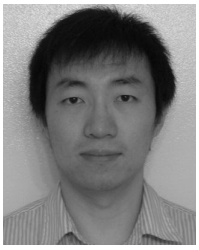

Xinyuan Chong received the B.S. and M.S. degrees in physics from Tsinghua University, in 2008 and 2011, respectively. He is currently pursuing the Ph.D. degree at the School of Electrical Engineering and Computer Science, Oregon State University. His current research interests include plasmonic-enhanced optical sensor for chemical detection, gas sensing, and biomedical applications.

Ki-Joong Kim received the Ph.D. degree in chemical engineering from Sunchon National University, Korea, in 2009. During his Ph.D. work, he focused on the synthesis and characterization of nanomaterials for environmental processes, such as adsorption processes and catalytic reactions using modified activated carbons, zeolites, and nanocatalysts. He is currently a Post-Doctoral Researcher with Oregon State University. His main work has been focused on synthesis of functional materials, such as nanocrystals, quantum dots, and metal-organic frameworks with ultrahigh surface area, and use them for energy and environmental applications, including photovoltaics, gas storage/separations, hydrogen storage, catalysts, luminescence, and gas sensing.

Paul R. Ohodnicki received the bachelor's degrees in engineering physics and economics from the University of Pittsburgh, in 2005, and the M.S. and Ph.D. degrees in materials science and engineering from Carnegie Mellon University (CMU), in 2006 and 2008, respectively. He is currently a Staff Scientist and the Team Leader of the Electrochemical and Magnetic Materials Team within the Functional Materials Development Division, National Energy Technology Laboratory. He is responsible for overseeing several major projects in the areas of functional sensor materials for power generation and sub-surface applications, including solid oxide fuel cells and unconventional resource recovery, such as shale gas as an advanced anode and cathode engineering in solid-oxide fuel cells through infiltration. His primary research interests are focused on studies of nanostructured and nanocomposite material systems with a particular emphasis on materials for sensors, power electronics, and energy conversion devices. Prior to his current role at the NETL, he was a Staff Scientist with the Chemistry and Surface Science Division from 2011 to 2013, and he also worked in a program management role for the Solid State Energy Conversion Alliance Program, in 2010, focused on the development and deployment of large-scale solid-oxide fuel cell technology. He also spent several years as a Research and Development Engineer at PPG Industries where he worked on a development team to successfully commercialize a new optical coating for large-area low emissivity architectural window applications. He has held a position as an Adjunct Faculty Member of the Materials Science and Engineering Department at CMU since 2011, where he is currently the Chair of the Energy Conversion and Storage Committee of TMS, and was recently appointed as an Associate Editor for the *Journal of Electronic Materials*. He has authored or co-authored approximately 60 technical publications and has submitted over 12 patent applications with four patents successfully issued to date.

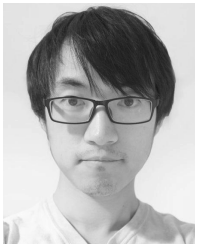

Erwen Li received the B.S. degree in physics from Fudan University, in 2011. He is currently pursuing the Ph.D. degree at the School of Electrical Engineering and Computer Science, Oregon State University. His current research interests include nanostructured photonic devices for sensing and spectroscopic application.

Chih-Hung Chang received the Ph.D. degree in chemical engineering from the University of Florida, Gainesville, FL, USA, in 1999. He is currently a Professor with the School of Chemical, Biological and Environmental, OSU. He established the Oregon Process Innovation Center for sustainable solar cell manufacturing, an Oregon BEST signature research facility, and serve as its Director. He is a SHARP Laboratories of America Scholar and a recipient of the NSF CAREER Award and Intel Faculty Fellowship. He has been serving as the PI or Co-PI for a number energy-related projects. His group has studied solution-based thin-film deposition processes, nanomaterials, solar cells, thin-film transistors, and microreactor. He has over 90 peer-reviewed journal publications, ten issued patents, and three pending patents in these areas. He is the Founder and acting Chief Science Officer of an OSU-spin out venture, CSD Nano, Inc.

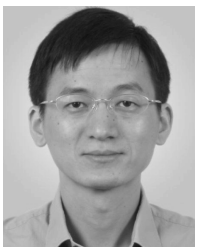

Alan X. Wang (SM'15) received the Ph.D. degree in electrical and computer engineering from The University of Texas at Austin, in 2006. He has been an Assistant Professor with the School of Electrical Engineering and Computer Science, Oregon State University, since 2011. From 2007 to 2011, he was with Omega Optics, Inc., where he served as the Chief Research Scientist for nine SBIR/STTR Projects. His research interests include nanophotonic devices for optical interconnects, and optical sensors for chemical and biological detection. His current research activities are sponsored by the National Science Foundation, the National Institutes of Health, the Oregon Nanoscience and Microtechnologies Institute, the National Energy Technology Laboratory, and industrial sponsors, such as Hewlett-Packard. He has over 50 journal publications and 50 conference presentations, and also holds three U.S. patents. He is a Senior Member of The Optical Society.